Corona Discharge – A Fully Coupled Numerical Approach Verified and Validated

D Rubinetti[1]*, D Weiss[1], W Egli[2]
1. Institute of Thermal and Fluid Engineering, University of Applied Sciences and Arts - Northwestern Switzerland
2. EGW Software Engineering

ABSTRACT
Corona discharge denotes the effect where an electrically non-conducting fluid is ionized under the influence of strong electrical fields in proximity of an emitting electrode. This technology is used in industry for a broad range of applications, e.g. the deposition of airborne particles. The electrodynamic nature of Corona discharge is often coupled with other physical phenomena, making it a key element of multiphysical problems. In order to accurately describe and set-up a model for Corona discharge processes a guideline is presented here. It can be implemented into codes which allow the user-input of custom partial differential equations. The governing equations of the approach developed are based on Maxwell's equations. The delicate part of calculating in an efficient way the electrical field distortion due to space charges is implemented by a Lagrange Multiplier, which allows the integrated identification of the unknown initial space charge density on the electrode. By means of a simplified test-case the results have been analytically verified. Additionally, the results of the modelling approach presented have been compared to experimental data available in literature, showing a good agreement.

1. INTRODUCTION

Corona discharge denotes a well-established technology to generate a continuous flow of ions in a fluid. The physical nature of the Corona discharge emerges from excess surface charges on a high-voltage electrode, which enables the charging of molecules of the surrounding fluid. In practice, the Corona discharge covers a broad range of applications that require an electrically conductive fluid. In the light of worldwide renewable energy promotion efforts, the Corona discharge plays its role as anti-pollution technology for exhaust gases. E.g. it allows the charging and deposition of airborne particles arising from combustion processes by electrostatic precipitation [1]. Further improvement of Corona discharge based devices preferably makes use of numerical modeling, to avoid or reduce elevated development costs of test rigs. For this purpose a robust modelling approach is presented and subsequently verified and validated in this study.

2. PHYSICAL MODEL

Corona discharge being an electrodynamic phenomenon, the governing equations are based on Maxwell's equations, assuming steady-state conditions without magnetic influence.

*Corresponding Author: donato.rubinetti@fhnw.ch

As a result from the combination of charge conservation condition with the charge transport equation, the Poisson-continuity coupled equations yield [1]

$$\nabla^2\phi = -\frac{\rho_{el}}{\varepsilon_0} \tag{1}$$

$$\vec{E}\nabla\rho_{el} = -\frac{{\rho_{el}}^2}{\varepsilon_0} \tag{2}$$

with ϕ being the electric potential, ρ_{el} the space charge density, ε_0 the vacuum permittivity and $\vec{E} = -\nabla\phi$ being the electric field.

Note that (2) is obtained when the contribution of a fluid flow velocity $\vec{u}$ to the electric current density $\vec{j} = \rho_{el}(b\vec{E} + \vec{u})$, where b denotes the ion mobility, can be neglected.

The two equations (1) to determine the electric potential ϕ, based on a known distribution of ρ_{el}, and (2) to determine the electric charge density ρ_{el}, based on a known distribution of ϕ and $\vec{E} = -\nabla\phi$, respectively, need to be supplemented by appropriate boundary conditions.

The equations (1) and (2) are coupled, their solutions are not independent from each other. In a similar way, the boundary conditions for ϕ and ρ_{el} will not be independent from each other. For numerical purposes, the boundary condition are frequently formulated such that the electric field is limited by some Corona onset field strength E_0, in addition to the boundary conditions of the Dirichlet type that apply already to determine the distribution of the electric potential. In this way, the electric field at the electrode surface is smaller than E_0 if ever no Corona is formed, i.e. when $\rho_{el} = 0$ at that point, whereas $|\vec{E}| = E_0$ at the electrode when $\rho_{el} \neq 0$. It seems that from the mathematical point of view, existence and uniqueness of the solution are not clear for general situations of this kind of problem; practical experience based on analytical and numerical solutions indicate, though, that solutions exist and appear to be unique, giving strong hints that the kind of boundary conditions outlined above is meaningful.

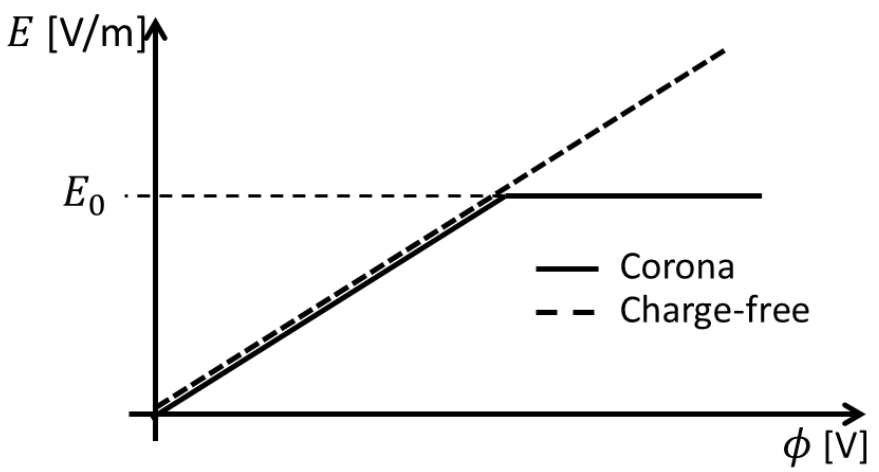

Figure 1: Physical interpretation and visualization of the Corona-onset field strength condition at the electrode

Figure 1 compares the boundary conditions at the electrode for the charge-free case without ionization processes with the Corona-case. An increasing electric potential gives a rise to the electric field strength up to the onset field strength E_0. Beyond that threshold Corona develops, maintaining the field strength constant.

The onset field strength E_0 , measured expressed in [V/m], is primarily determined by the shape of the emitting electrode with the empirical correlation [1][6]

$$E_0\left[\frac{V}{m}\right] = 3 \times 10^6 f_r \left(m_s + 0.03\sqrt{\frac{m_s}{r_E[m]}}\right) \tag{3}$$

where f_r is a dimensionless fatigue estimation ($f_r = 0.6$ for practical use), m_s denotes the relative gas density and $r_E[m]$ the radius of the emitting electrode, measured in [m].

From the physical point of view, the notion is emphasized that the domain of interest will be set up by two parts, one of which is characterized by $\rho_{el} = 0$, and the other part by $\rho_{el} \neq 0$, containing all the streamlines of the electric current density $\vec{j}$. These streamlines start from points on the electrode where Corona occurs, cf. Figure 2.

3. NUMERICAL MODEL

The numerical model approach described in this study is based on the interdependance of equations (1) and (2). Equation (1), by the boundary conditions outlined above, on a first view appears overdetermined, whereas (2), due to the lack of an information with respect to the charge density on the electrode, appears underdetermined. Therefore an appropiate workaround formulation by means of a Lagrange multiplier is implemented.

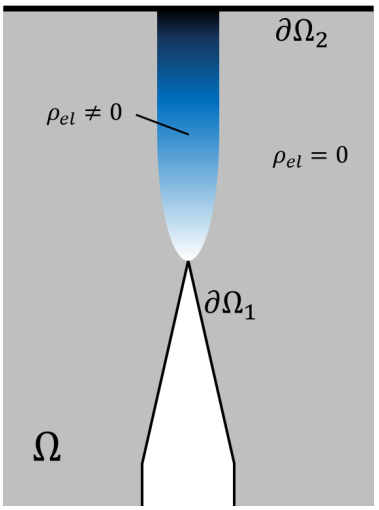

Figure 2: Representative 2D-sketch for the numerical model including an emitting electrode and a plate. The notion is that the domain consists of a part with vanishing charge density, and a domain where $\rho_{el} \neq 0$. The latter is set up by the streamlines of the current density $\vec{j}$ starting from places on the electrode where Corona occurs.

3.1 General Setup

For successful convergence of the Corona calculation a two-step setup is recommended:

1) Stationary calculation of the field for the charge-free, i.e. the Laplace case
2) Poisson-coupled calculation of Corona

The former is rather straightforward, it is described in Section 3.2. The latter is somewhat more delicate, it is described in Section 3.3.

Table 1: Summary of the required boundary conditions and initial values for the charge-free case to determine the initial solution

Entity	**PDE (1)**	**PDE (2)**	**Initial Value for ϕ**
$\partial\Omega_1$	Dirichlet type: Electric potential ϕ_1	n/a	
$\partial\Omega_2$	Dirichlet type: Electric potential ϕ_2	n/a	
Ω			0

3.2 Steady charge-free electric field

Table 1 summarizes the relevant boundary and initial conditions to numerically investigate the charge-free case. This preliminary step reduces equation (1) to a Laplace equation by assuming a non-emitting electrode, therefore $\rho_{el} = 0$ everywhere, and equation (2) is trivially satisfied in this step and does not need to be solved numerically. Two Dirichlet boundary conditions are used for the electric potential on the electrodes. The result of this calculation leads to a first guess for the electric field.

3.3 Poisson-coupled calculation of Corona

The resulting electric field from the previous step is taken as initial value for the Corona calculation to avoid the trivial zero solution for the space charge density. Table 2 summarizes the boundary conditions and initial values used in this second step. As introduced above, particular attention needs to be given to the boundary conditions for the emitting electrode. To obtain a well-posed problem, equation (1) demands two boundary conditions, whereas equation (2) asks for an a priori unknown value for the space charge density on the electrode. Due to the nature of equation (2), no additional boundary condition is to be given on the opposite electrode $\partial\Omega_2$.

To determine the unknown value of ρ_{el} on $\partial\Omega_1$ an approach with a Lagrange Multiplier is recommended. In order to do so, it is necessary to split the space charge density variable into a space-dependent part $\rho_{el,sp}$ for the transport equation and a constant variable $\rho_{el,c}$ which represents the dirichlet boundary condition for the transport equation [3]. The following list provides a step-by-step modelling guide for the boundary conditions setup for a fully coupled Corona calculation:

1) Define electric potential ϕ_2 on $\partial\Omega_2$ (as a Dirichlet BC).
2) Define electric displacement field on the electrode $-\varepsilon_0 E_0 \vec{n}$ (as a Neumann type of BC).
3) Enforce constraint for the electric potential on the electrode $\phi|_{\partial\Omega_1} = \phi_1$, i.e. the Dirichlet type BC.
4) Define Lagrange Multiplier $\rho_{el,c}$ to ensure the given constraint for the electric potential is respected.
5) Set $\rho_{el,c}$ as Dirichlet BC for the transport equation (2).

Steps 1) to 5) ensure the fully coupled solving process. In detail, Points 3) and 4) are the key elements of the coupling, as they loop the dependent variable for the electric potential ϕ in equation (1) in an iterative way. On the electrode an electric potential $\phi = \phi_1$ and an electric field E_0 are enforced. Consequently, the constant space charge density $\rho_{el,c}$ - acting as Lagrange Multiplier - bridges the occurring discrepancy and interdependency of the given values.

Table 2: Summary of the required boundary conditions and initial values for the Corona-discharge problem

Entity	**PDE (1)**	**PDE (2)**	**Initial Value for ϕ**
$\partial\Omega_1$	Neumann type: $-\varepsilon_0 E_0 \vec{n}$	Dirichlet type: $\rho_{el,c}$	
$\partial\Omega_2$	Dirichlet type: Electric potential ϕ_2	n/a	
Ω			$\phi_{initial}$

3.4 Mesh

Figure 3 shows the geometry cutout in electrode proximity, for an electrode with tip radius 0.15 mm. It is recommended to wrap the emitting electrode in boundary layers to handle the sharp gradients of the electric field. In this case, the thickness of the cell layer closest to the wall amounts to about 0.0015 times the radius of the electrode tip.

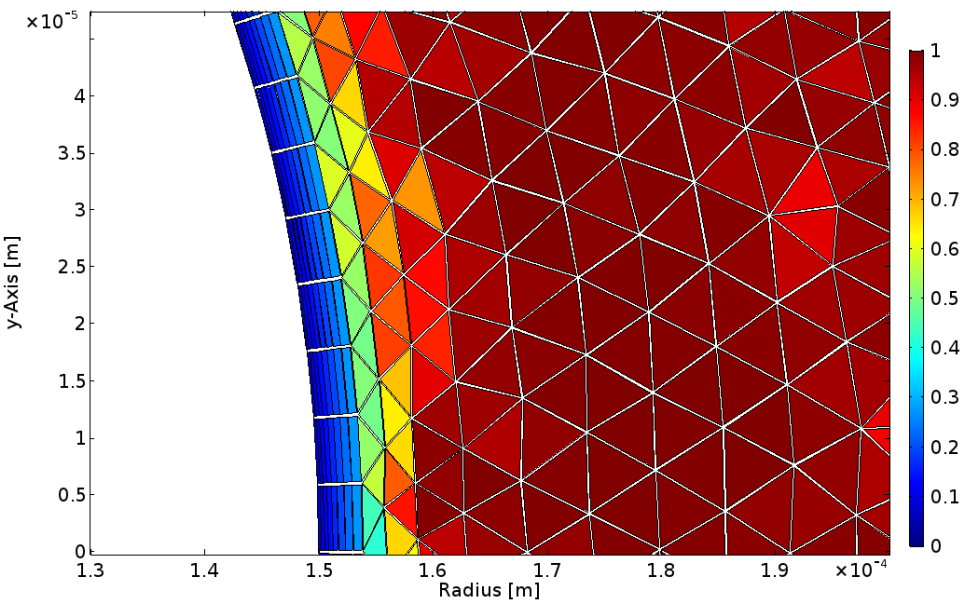

Figure 3: Mesh cutout in electrode proximity. The color legend is based on the element quality, which is at its lowest on the electrode due to large aspect ratios.

4. ANALYTICAL VERIFICATION

The numerical model is verified with a simplified test-case that includes two concentrically arranged spheres according to figure 4, with an outer to inner sphere radius ratio of $R_2/R_1 = 150$.

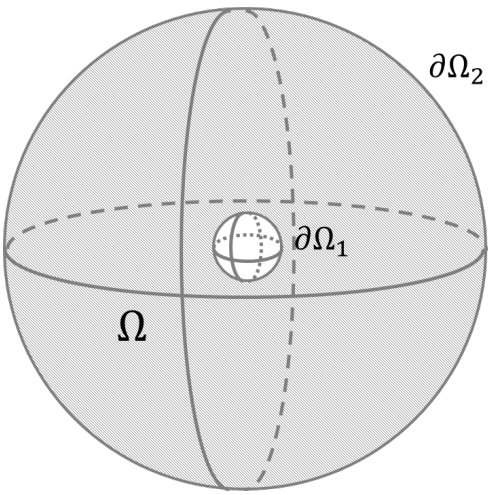

Figure 4: Simplified test-case geometry. The inner sphere is shown enlarged for illustration purposes.

In this case the inner sphere represents the emitting electrode $\partial\Omega_1$ with an electric potential of $\phi_1 = 10kV$, whereas the outer electrode is set to ground.

Figure 5 shows the numerical result for the space charge density within the computed cross section. The direct comparison between the charge-free case and Corona discharge can be observed in figure 6. Due to the influence of the space charges the electric potential expands.

For the simplified test-case geometry presented, analytical correlations for the dimensionless electric field $\hat{E}$ and space charge density $\hat{\rho}_{el}$ along the dimensionless radius $\hat{r} = \frac{r}{r_E}$ can be derived as [4]

$$\frac{E(r)}{E_0} = \hat{E}(\hat{r}) = \frac{1}{\hat{r}^2}\sqrt{1 + \hat{A}(\hat{r}^3 - 1)} \tag{4}$$

$$\frac{\rho_{el}(r)}{\frac{\varepsilon_0 E_0}{r_E}} = \hat{\rho}_{el}(\hat{r}) = \frac{3\hat{A}}{2\sqrt{1+\hat{A}(\hat{r}^3-1)}} \tag{5}$$

with the dimensionless current $\hat{A}$:

$$\hat{A} = \frac{I}{6\pi\varepsilon b \cdot {E_0}^2 \cdot r_E} \tag{6}$$

Where I denotes the dimensional (integral) electrical current and ε the relative permittivity. As shown by the plots in figures 7 and 8 the numerical and analytical solutions are identical.

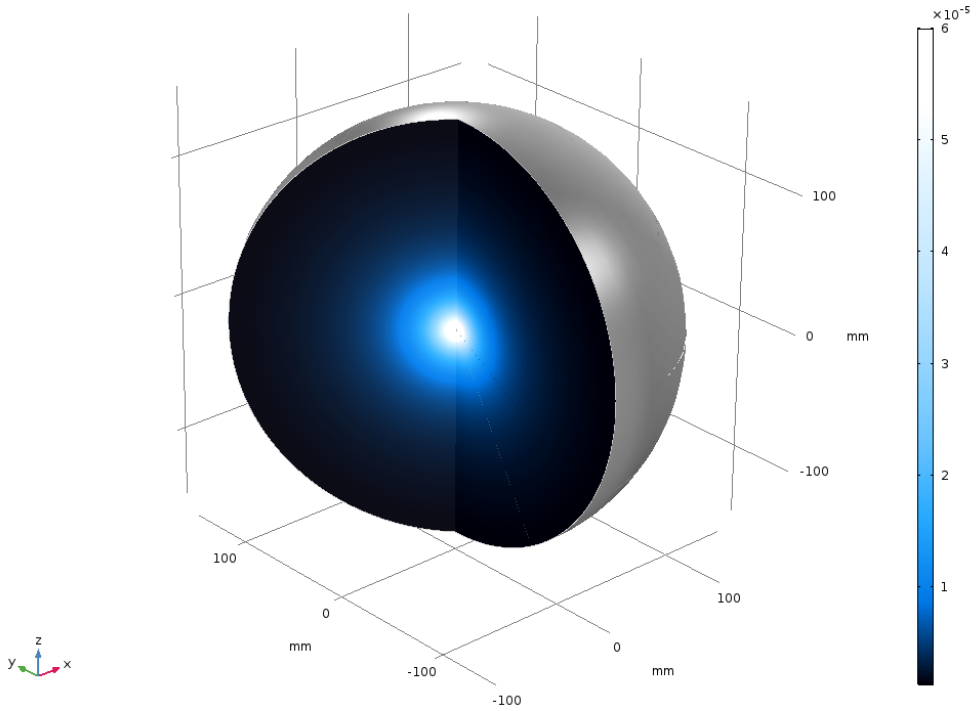

Figure 5: Result for the space charge density [C/m^3]

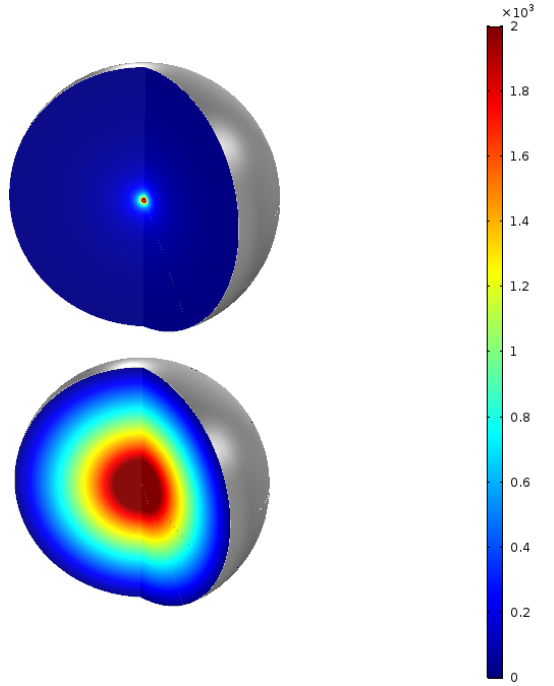

Figure 6: Direct comparison of the charge-free case (top) and the Corona discharge case (bottom) for the electric potential in [V]

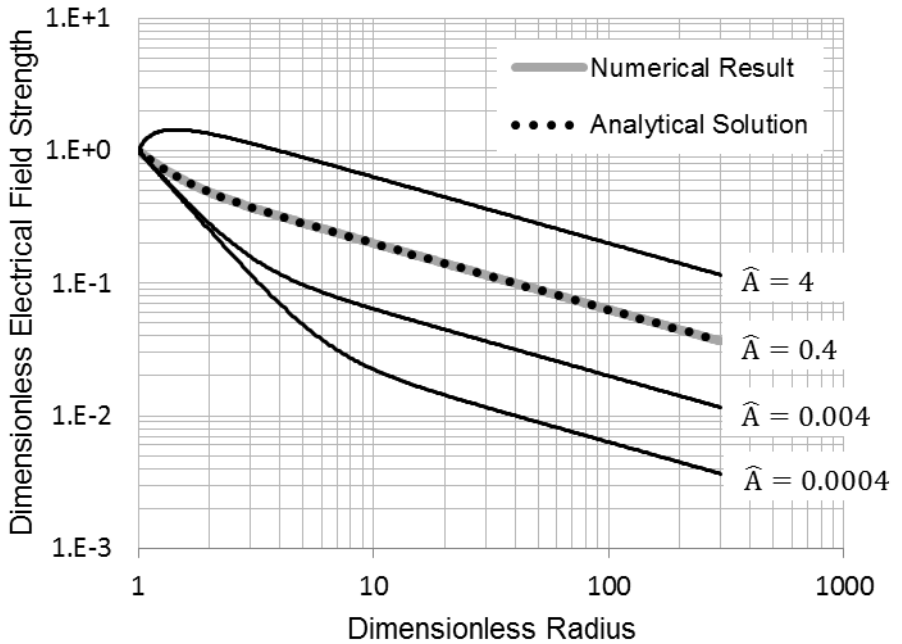

Figure 7: Analytical verification of the electric field along the radius for several values of $\hat{A}$. The field strength scales as $\hat{r}^{-1/2}$ for large $\hat{r}$. Curves corresponding to further values for the dimensionless current are plotted for comparison.

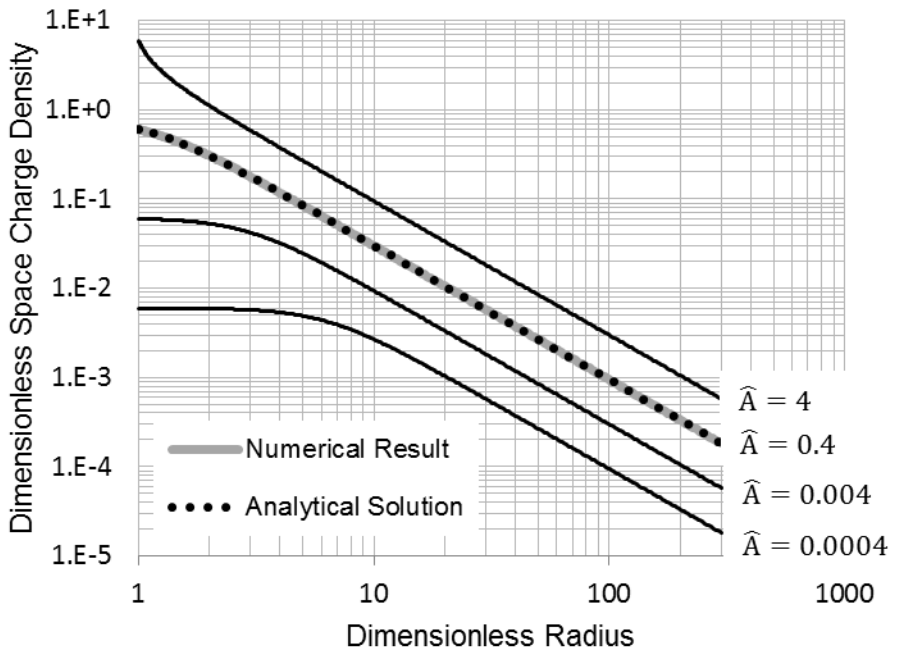

Figure 8: Analytical verification of the space charge density along the radius for several values of $\hat{A}$. The charge density scales as $\hat{r}^{-3/2}$ for large $\hat{r}$. Curves corresponding to further values for the dimensionless current are plotted for comparison.

5. EXPERIMENTAL VALIDATION

The present concept for the calculation of Corona discharge is numerically robust and accurate. It can be applied to other geometries using the same methodology. Figure 9 shows an experimental setup for the measurement of local electrical quantities [5]. It consists of an emitting needle and a grounded plate. In this experiment the electrical field strength, the space charge density, and the electric potential have been measured.

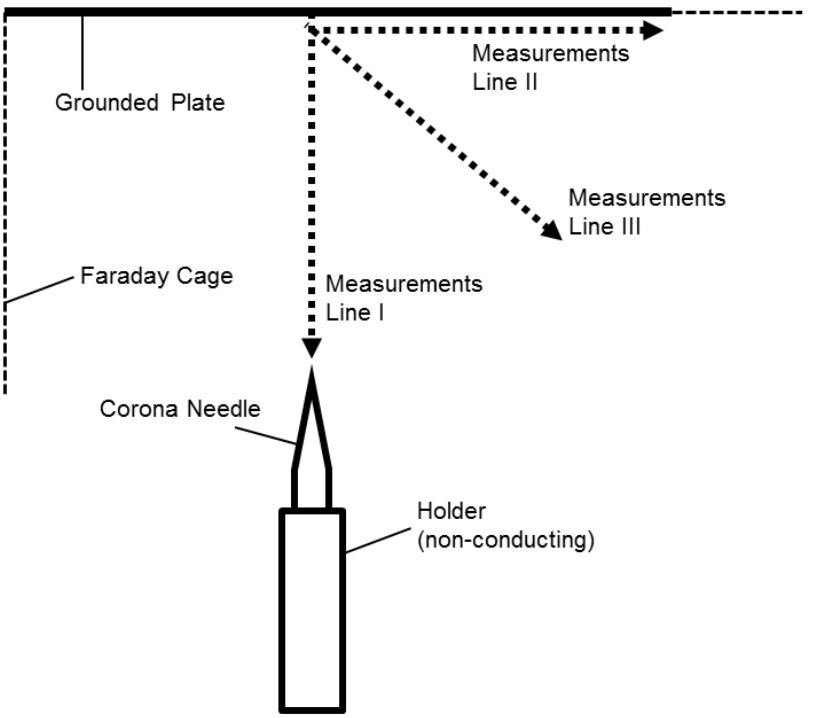

Figure 9: Experimental setup used in [7]

Figures 10 and 11 compare the results obtained with the present modeling concept to the data from the 2005 experiment [5,6]. It can be seen that the experimental and numerical data are in close agreement. One exception refers to the measurement of the electric field on line 1 towards the needle. The simulation correctly represents the sharp gradient of the electric field, whereas the measurement cannot handle the significant increase. Taking the limits of measurement devices into account, it can be stated that the analytical verification is an appropiate approach to confirm the calculations.

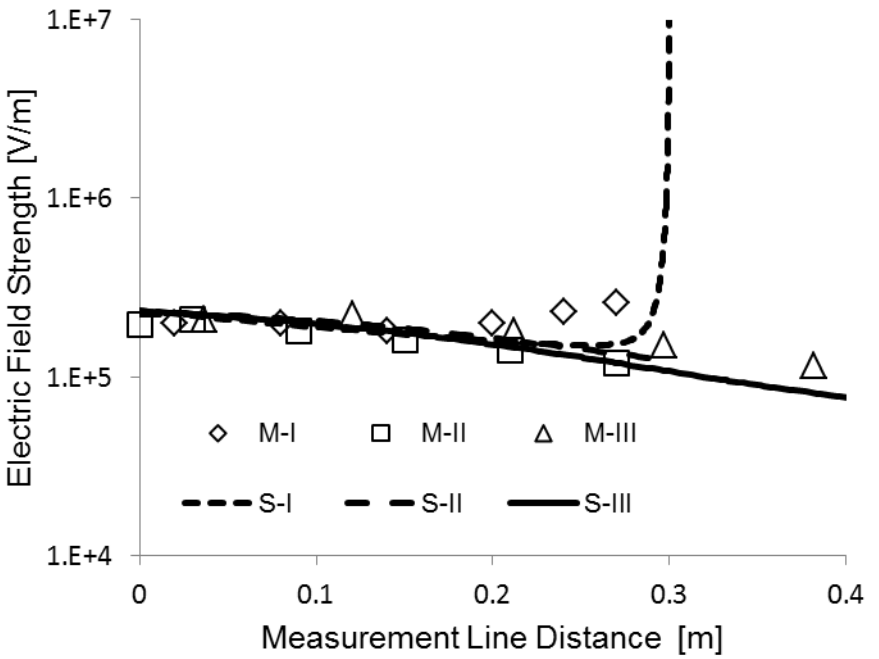

Figure 10: Comparison of simulation results (S) and measurements (M) for the electric field for each measurement line (I-III)

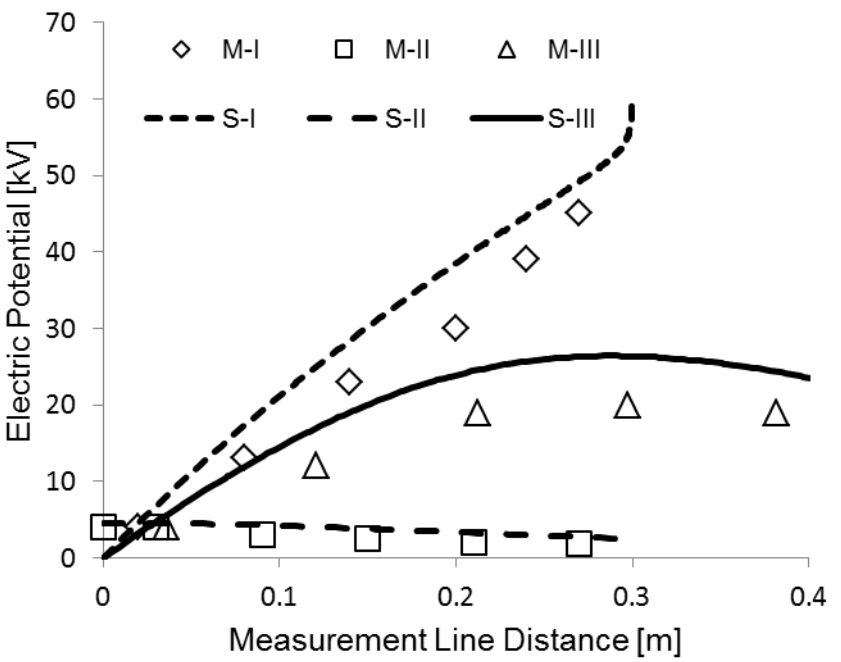

Figure 11: As integral quantity, the experimental data shows closer agreement with the simulation

6. CONCLUSION

The numerical model presented to compute common Corona discharge problems is physically correct and numerically stable. By means of a Lagrange Multiplier the unknown bounday condition for the space charge density on the electrode can be computed within the set of governing equations using a constraint for the electric potential. Representation of steep electrical field gradients in close proximity to the electrode requires a fine grid resolution, a fact which can lead to significant computational efforts for complex cases and 3D models. The model presented has been tested for two different geometries, and its results have been verified with a test-case and compared to measurement data. This approach to model Corona discharge problems can be seamlessly transferred to other related applications.

REFERENCES

[1] Rubinetti, D.; Weiss, D. A.; Egli, W. (2015). Electrostatic Precipitators – Modelling and Analytical Verification Concept, University of Applied Sciences Northwestern Switzerland, Windisch, Switzerland, COMSOL Conference 2015, Grenoble 14-16 October.

[2] White, Harry J. (1963): Industrial electrostatic precipitation. Pergamon.

[3] Favre, Eric (2013): Coronal with details/Corona discharge problem. http://www.comsol.com/community/forums/general/thread/14399 , accessed on 2017-05-18.

[4] Weiss, D. A. (2014): Notes on electrostatics and fluid mechanics. University of Applied Sciences and Arts - Northwestern Switzerland.

[5] Meyer, J.; Marquard, A.; Poppner, M.; Sonnenschein, R. (2005): Electric Fields coupled with ion space charge. Part 1: Measurements. Journal of Electrostatics, Volume 63, p.775-780.

[6] Poppner, M.; Meyer, J.; Sonnenschein, R. (2005): Electric Fields coupled with ion space charge. Part 2: computation. Journal of Electrostatics, Volume 63, p. 781-787.